

Article

Synthesis of Reusable Silica Nanosphere-Supported Pt(IV) Complex for Formation of Disulfide Bonds in Peptides

Xiaonan Hou, Xiaowei Zhao, Yamei Zhang, Aiying Han, Shuying Huo*, and Shigang Shen*

College of Chemistry and Environmental Science, Key Laboratory of Analytical Science and Technology of Hebei Province, and the MOE Key Laboratory of Medicinal Chemistry and Molecular Diagnostics, Hebei University, No 180, Wusi Dong Roald, Baoding 071002, Hebei Province, P. R. China; 18233272151@163.com (X.H.); wjswbys@126.com (X.Z.); 15231212708@163.com (Y.Z.); 739095567@qq.com (A.H.)

*Correspondence: shuyinghuo@126.com; Tel.: +86-312-5079386; shensg@hbu.edu.cn; Tel.: +86-312-5079386

Abstract: Some peptide-based drugs including oxytocin, vasopressin, ziconotide, pramlintide, nesiritide, and octreotide, contain one intramolecular disulfide bonds. A novel and reusable monodispersed silica nanosphere-supported Pt(IV) complex ($\text{SiO}_2@\text{TPEA}@\text{Pt(IV)}$) was synthesized via a four-step procedure and used for formation of intramolecular disulfide bonds in peptides. TEM and chemical mapping results for the Pt(II) intermediates and for $\text{SiO}_2@\text{TPEA}@\text{Pt(IV)}$ show that the silica nanospheres possess a monodisperse spherical structure and contain uniformly distributed Si, O, C, N, Cl, and Pt. The valence state of Pt on the silica nanospheres was characterized by XPS. The Pt(IV) loaded on $\text{SiO}_2@\text{TPEA}@\text{Pt(IV)}$ was 0.15 mmol/g, as determined by UV-vis spectrometry. Formation of intramolecular disulfides in six dithiol-containing peptides of variable lengths by use of $\text{SiO}_2@\text{TPEA}@\text{Pt(IV)}$ was investigated and the relative oxidation yields were determined by HPLC. In addition, peptide **1** (Ac-CPFC-NH₂) was utilized to study the reusability of $\text{SiO}_2@\text{TPEA}@\text{Pt(IV)}$. No significant decrease in the relative oxidation yield was observed after ten reaction cycles. Moreover, the structure of $\text{SiO}_2@\text{TPEA}@\text{Pt(IV)}$ after being used ten cycles was determined to be similar to its initial one, demonstrating the cycling stability of the complex.

Keywords: monodisperse silica nanospheres; supported platinum(IV) complex; peptide; intramolecular disulfide; reusability

1. Introduction

A big fraction of the peptide-based drugs available in the market, including oxytocin, vasopressin, ziconotide, pramlintide, nesiritide, and octreotide, contain one or multiple intramolecular disulfide bonds. Disulfide bonds play a crucial role in both the structural and functional properties of the peptides, providing enhanced stability, selectivity, and potency [1-4]. Thus, the efficient formation of disulfide bonds is an important step in the synthesis of peptide-based drugs. Oxidation of suitable thiol-containing peptides in solution by oxidants such as air, dimethyl sulfoxide, iodine, and hydrogen peroxide is a common procedure for disulfide formation. However, the oxidation process using these oxidants often suffers from several drawbacks including low yield, long reaction time, and formation of side products due to over-oxidation or oxidation of Met, Trp, and Tyr residues [5-9]. Therefore, a high research interest is to develop new and efficient oxidants which are suitable to the disulfide formation. In this context, some efficient oxidants such as *trans*-[PtCl₂(CN)₄]²⁻ and *trans*-[PtCl₂(en)₂]²⁺, dihydroxyselenolane oxide (DHX^{ox}), and N-chlorosuccinimide (NCS) have been developed and utilized for the formation of disulfide bonds in peptides [10-18].

Alternately, the use of solid-supported oxidants has also been investigated for disulfide formation because these oxidants possess favorable properties such as reusability, mild reaction

conditions, as well as a “pseudo-dilution” effect. So far, three types of solid-supported oxidants including polymer-supported Ellmans’ reagent (Clear-Ox), polymer-supported oligomethionine sulfoxide (Oxyfold reagent), and ChemMatrix-supported NCS have been developed [19-22]. It has been found that at least a ten time excess of Clear-Ox must be used because of the thiol-disulfide exchange properties in peptides [19]. While high purity disulfide bonds have been obtained with Oxyfold reagent and ChemMatrix-supported NCS, the reusability of the two oxidants has not yet been explored [20,21].

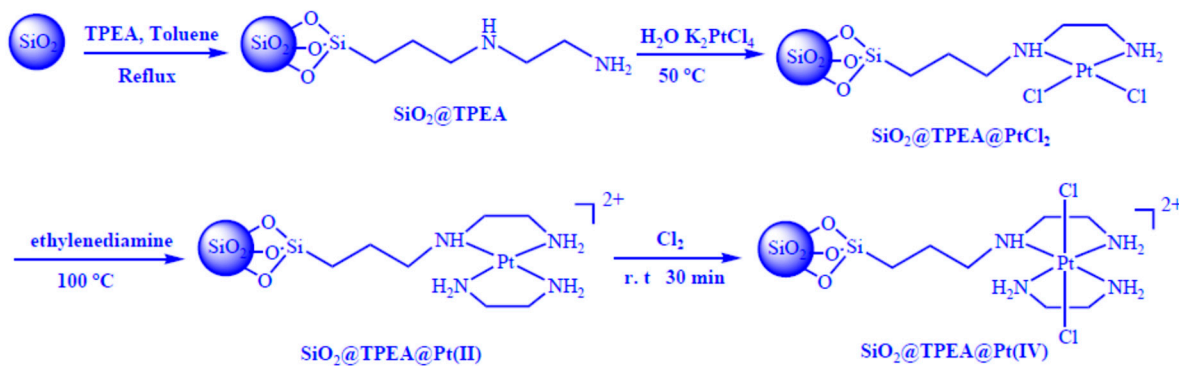
Recently, silica nanospheres have been used successfully as a solid support in the preparation of recyclable and reusable catalysts for organic synthesis, because they possess the properties of high surface area, high thermal stability, and variability in structures [23-28]. In addition, they can be simply prepared by Stober method and functionalized by reacting with various types of coupling agents [29,30].

In this work, we have designed and synthesized a silica nanosphere-supported platinum(IV) complex as a novel solid-supported oxidant and have used for disulfide formation in several dithiol-containing peptides of variable lengths. The solid-supported oxidant was characterized by transmission electron microscopy (TEM), elemental analysis, X-ray photoelectron spectroscopy, and scanning electron microscopy (SEM) techniques. Further, the oxidant can be used in various buffer solutions, exhibiting an excellent durability; and it can be reused several times without change in its morphology.

2. Results and discussion

2.1. Synthesis and characterization of $\text{SiO}_2@\text{TPEA}@\text{Pt(IV)}$

$\text{SiO}_2@\text{TPEA}@\text{Pt(IV)}$ was synthesized via the following four-step procedure, which is illustrated in Scheme 1: preparation of $\text{SiO}_2@\text{TPEA}$ by the functionalization of SiO_2 with TPEA; complexation of $\text{SiO}_2@\text{TPEA}$ with K_2PtCl_4 to give $\text{SiO}_2@\text{TPEA}@\text{PtCl}_2$; preparation of $\text{SiO}_2@\text{TPEA}@\text{Pt(II)}$ through the reaction of ethylenediamine with $\text{SiO}_2@\text{TPEA}@\text{PtCl}_2$; and preparation of $\text{SiO}_2@\text{TPEA}@\text{Pt(IV)}$ by the oxidation of $\text{SiO}_2@\text{TPEA}@\text{Pt(II)}$ using chlorine gas.



Scheme 1. A schematic route for synthesis of $\text{SiO}_2@\text{TPEA}@\text{Pt(IV)}$.

A TEM image of SiO_2 is shown in Figure S1. Analysis of the image revealed that SiO_2 possessed a monodisperse spherical structure with an average diameter of about 420 nm. After modification of SiO_2 by TPEA, the produced $\text{SiO}_2@\text{TPEA}$ had a white color, and its morphology was unchanged compared to the parent SiO_2 (see Figure S1 in Supporting Information). To confirm the presence of TPEA on the SiO_2 surface, FT-IR spectra of pure SiO_2 and $\text{SiO}_2@\text{TPEA}$ were compared (Figure S2); a weak band was observed at 2922.2 cm^{-1} for $\text{SiO}_2@\text{TPEA}$, which was not found in the case of pure SiO_2 . This band can be assigned to the aliphatic $-\text{CH}_2$ stretching vibration originated from the propyl chain in TPEA, confirming the presence of TPEA on the SiO_2 surface [31]. Moreover, a significant reduction in the $\text{Si}-\text{OH}$ stretching vibration peak intensity at 944.4 cm^{-1} was observed, illustrating that the

surface Si–OH groups on SiO_2 exchanged with the methoxy groups in TPEA during surface modification [32,33].

$\text{SiO}_2@\text{TPEA}@\text{PtCl}_2$ had brown color, and its morphology and chemical element distribution were investigated using TEM and TEM coupled with chemical mapping, respectively. As shown in Figure 1a, $\text{SiO}_2@\text{TPEA}@\text{PtCl}_2$ particles also possess a monodisperse spherical structure. Moreover, Si, O, C, elements have a uniform distribution on the surface, conforming to the presence of TPEA on the SiO_2 nanospheres. Cl and Pt are also present on $\text{SiO}_2@\text{TPEA}@\text{PtCl}_2$, demonstrating that the $-\text{NHCH}_2\text{CH}_2-\text{NH}_2$ group in TPEA reacted with K_2PtCl_4 forming $\text{SiO}_2@\text{TPEA}@\text{PtCl}_2$ [34,35]. Ethylenediamine was used to substitute the two coordinated chlorides in $\text{SiO}_2@\text{TPEA}@\text{PtCl}_2$ [36–38], giving rise to $\text{SiO}_2@\text{TPEA}@\text{Pt(II)}$. The morphology $\text{SiO}_2@\text{TPEA}@\text{Pt(II)}$ is shown in Figure 1b. A corona-like structure is found for $\text{SiO}_2@\text{TPEA}@\text{Pt(II)}$; but this structure was not found for $\text{SiO}_2@\text{TPEA}@\text{PtCl}_2$.

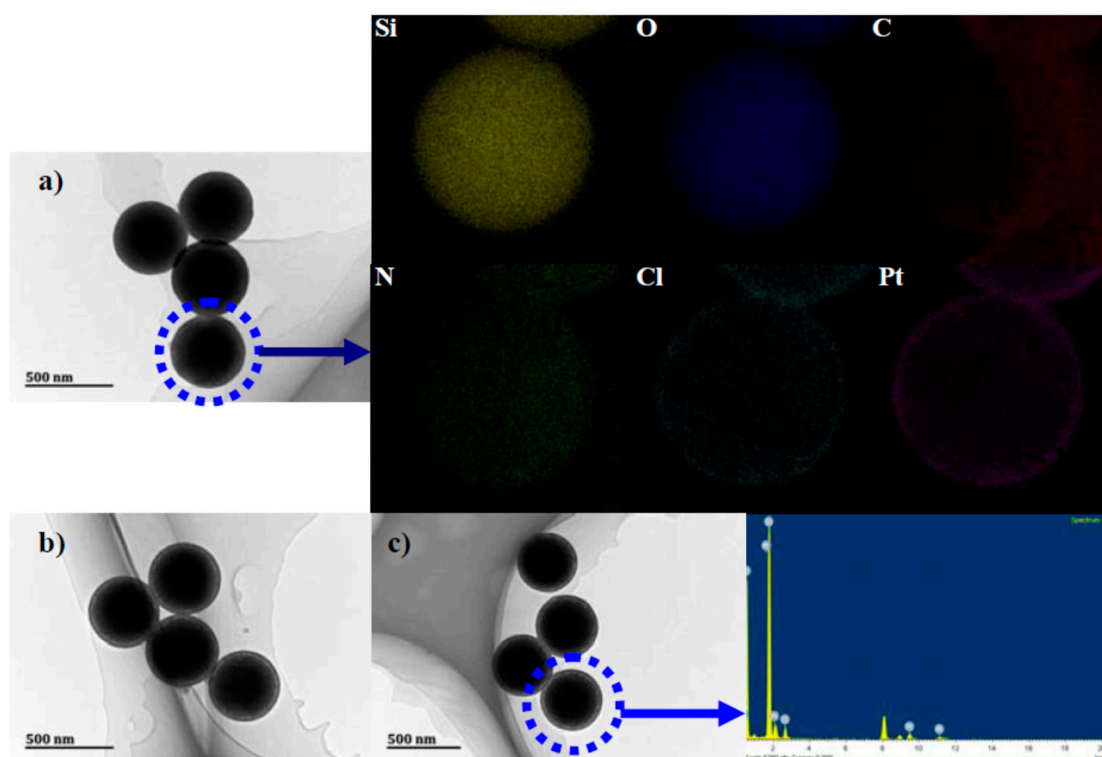


Figure 1. (a) TEM image and elemental mapping of $\text{SiO}_2@\text{TPEA}@\text{PtCl}_2$. (b) TEM image of $\text{SiO}_2@\text{TPEA}@\text{Pt(II)}$. (c) TEM image and EDX data for $\text{SiO}_2@\text{TPEA}@\text{Pt(IV)}$.

For the synthesis of $\text{SiO}_2@\text{TPEA}@\text{Pt(IV)}$, chlorine gas was used as the oxidant because the silica nanospheres are inert to chlorine gas [39,40]. The loading of the Pt(IV) complex did not increase with the raise of the oxidation time. The morphology and EDX data of $\text{SiO}_2@\text{TPEA}@\text{Pt(IV)}$ are shown in Figure 1c. The EDX data suggests that the N to Pt atomic ratio on the surface of the material is about 4:1. The N and Pt loadings on $\text{SiO}_2@\text{TPEA}@\text{Pt(IV)}$ were determined by elemental analysis and ICP-MS, respectively and were found to be 1.10 mmol and 0.21 mmol/g, respectively.

The XPS spectra recorded for $[\text{Pt}(\text{en})_2]\text{Cl}_2$, $[\text{PtCl}_2(\text{en})_2]\text{Cl}_2$, $\text{SiO}_2@\text{TPEA}@\text{Pt(II)}$, and $\text{SiO}_2@\text{TPEA}@\text{Pt(IV)}$ are shown in Figure 2. As seen in the figure, the two peaks corresponding to $\text{Pt(II)}_{4f(5/2)}$ and $\text{Pt(II)}_{4f(7/2)}$ are centered at binding energy values of 76.62 and 73.38 eV, respectively, in the XPS spectrum of $[\text{Pt}(\text{en})_2]\text{Cl}_2$. In the case of $[\text{PtCl}_2(\text{en})_2]\text{Cl}_2$, three peaks are observed at 79.70, 76.62, and 73.63 eV. This is because $[\text{PtCl}_2(\text{en})_2]\text{Cl}_2$ is partially reduced by X-rays during the XPS experiments [41,42]. The peaks at 79.70 and 73.63 eV are assigned to $\text{Pt(IV)}_{4f(5/2)}$ and $\text{Pt(II)}_{4f(7/2)}$, respectively, whereas the peak at 76.62 eV is assigned to the overlapped $\text{Pt(II)}_{4f(5/2)}$ and $\text{Pt(IV)}_{4f(7/2)}$ peaks [43]. In the case of $\text{SiO}_2@\text{TPEA}@\text{Pt(II)}$, two peaks corresponding to $\text{Pt(II)}_{4f(5/2)}$ and $\text{Pt(II)}_{4f(7/2)}$ are observed at 76.56 and 73.23 eV, respectively. Compared to the XPS spectrum of $[\text{Pt}(\text{en})_2]\text{Cl}_2$, the

$\text{Pt(II)}_{4\text{f}(5/2)}$ and $\text{Pt(II)}_{4\text{f}(7/2)}$ peaks are shifted in the negative binding energy direction in the case of $\text{SiO}_2@\text{TPEA}@\text{Pt(II)}$. These negative shifts may be attributed to different complexation mechanisms in the two platinum complexes [44]. Further, three peaks at binding energies of 79.49, 76.66, and 73.483 eV are observed in the XPS spectrum of $\text{SiO}_2@\text{TPEA}@\text{Pt(IV)}$, which are similar to the peaks observed for $[\text{Pt}(\text{en})_2\text{Cl}_2]\text{Cl}_2$. Furthermore, compared to the XPS spectrum of $\text{SiO}_2@\text{TPEA}@\text{Pt(II)}$, a new peak at a binding energy of 79.56 eV is observed in the XPS spectrum of $\text{SiO}_2@\text{TPEA}@\text{Pt(IV)}$, which is assigned to $\text{Pt(IV)}_{4\text{f}(5/2)}$. This demonstrates that $\text{SiO}_2@\text{TPEA}@\text{Pt(II)}$ was oxidized successfully to $\text{SiO}_2@\text{TPEA}@\text{Pt(IV)}$ by chlorine gas.

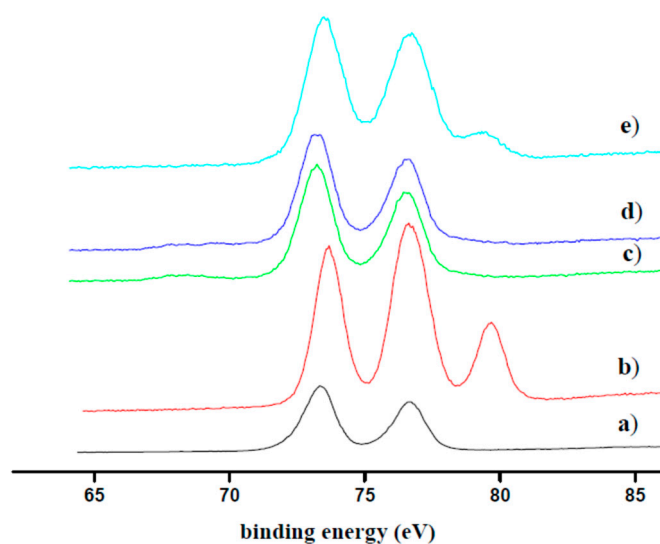


Figure 2. High resolution Pt 4f XPS spectra of (a) $\text{Pt}(\text{en})_2\text{Cl}_2$, (b) $[\text{Pt}(\text{en})_2\text{Cl}_2]\text{Cl}_2$, (c) $\text{SiO}_2@\text{TPEA}@\text{Pt(II)}$, (d) $\text{SiO}_2@\text{TPEA}@\text{Pt(II)}$ generated from the peptide **1** reduction of $\text{SiO}_2@\text{TPEA}@\text{Pt(IV)}$, and (e) $\text{SiO}_2@\text{TPEA}@\text{Pt(IV)}$.

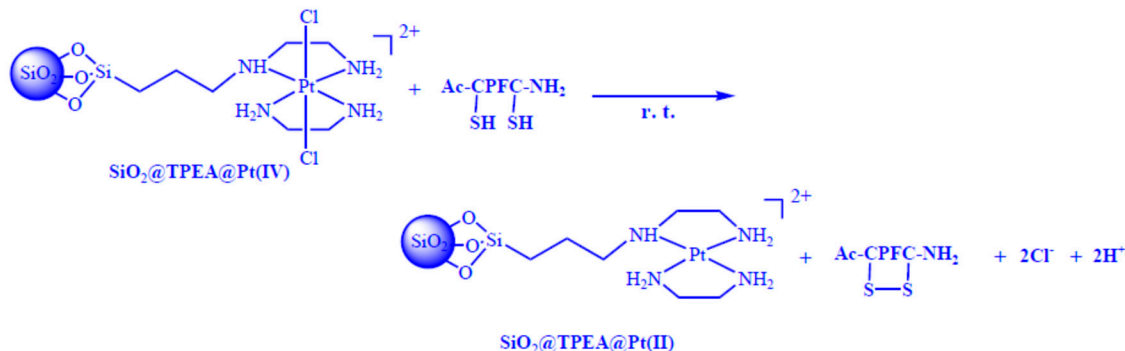
2.2. Pt(IV) loading determination of $\text{SiO}_2@\text{TPEA}@\text{Pt(IV)}$

2,5-Dimethoxythiophenol has been used for determining the loading of immobilized NCS as described the literature [22]. However, the reaction between $[\text{Pt}(\text{en})_2\text{Cl}_2]\text{Cl}_2$ and 2,5-dimethoxythiophenol has not yet been studied. Therefore, the stoichiometric ratio between *trans*- $[\text{PtCl}_2(\text{en})_2]^{2+}$ and 2,5-dimethoxythiophenol was determined in this work. A plot of absorbance versus $[\text{PtCl}_2(\text{en})_2]^{2+}$ is presented in Figure S3, which shows that the data points follow two straight lines. The stoichiometric ratio of $[\text{PtCl}_2(\text{en})_2]^{2+}/[\text{2,5-dimethoxythiophenol}]$ was estimated to be 1:1.8. This stoichiometric ratio implies that 2,5-dimethoxythiophenol was mainly oxidized to form a 2,5-dimethoxythiophenol dimer linked by a disulfide, which was confirmed by ESI-MS (observed $[\text{M} + \text{Na}]^+$ *m/z* 361.2). The same oxidation product was observed when 2,5-dimethoxythiophenol was oxidized by $\text{SiO}_2@\text{TPEA}@\text{Pt(IV)}$. Thus, we used the reaction between 2,5-dimethoxythiophenol and an excess of $[\text{Pt}(\text{en})_2\text{Cl}_2]\text{Cl}_2$ to construct a calibration curve which can be employed to determine the loading of $\text{SiO}_2@\text{TPEA}@\text{Pt(IV)}$. The calibration curve is shown in Figure S4. The Pt(IV) complex loading was determined to be 0.15 mmol/g.

2.3. Intramolecular disulfide formation in peptides by $\text{SiO}_2@\text{TPEA}@\text{Pt(IV)}$

Dithiol-containing peptides with variable lengths that were used in this work are listed in Table 1; their corresponding oxidized forms containing a disulfide ring vary in size from 14 to 38 atoms. The result of the reaction between peptide **1** and $\text{SiO}_2@\text{TPEA}@\text{Pt(IV)}$ is shown in Figure 3. A comparison of the chromatograms (Fig. 3a and Fig. 3b) shows that peptide **1** was oxidized thoroughly by $\text{SiO}_2@\text{TPEA}@\text{Pt(IV)}$ to its oxidized form. Details of the reaction conditions and MS spectra are provided in the Supporting Information. The reaction mechanism is illustrated in Scheme 2, similar

to that proposed earlier for the reactions between $[\text{Pt}(\text{en})_2\text{Cl}_2]\text{Cl}_2$ and the dithiol-containing peptides [10-14].



Scheme 2. Proposed mechanism for disulfide formation in peptide **1** by $\text{SiO}_2\text{@TPEA@Pt(IV)}$.

Previously, *trans*- $[\text{PtCl}_2(\text{en})_2]^{2+}$ was found to be a highly selective and efficient reagent for the rapid and quantitative formation of disulfide bonds in peptides [11]; no side reactions on the side chains of tryptophan, tyrosine and methionine, and no dimers formed through an intermolecular disulfide link were observed with the Pt(IV) complex [11]. Therefore, the peak area of oxidized peptide generated by *trans*- $[\text{PtCl}_2(\text{en})_2]^{2+}$ oxidation was used as a reference for investigating the efficiency of $\text{SiO}_2\text{@TPEA@Pt(IV)}$ for formation of disulfide bonds in peptides. The relative oxidation yield is defined by S_A/S_B , where S_A refers to the peak area corresponding to oxidized peptide **1** generated by the oxidation of $\text{SiO}_2\text{@TPEA@Pt(IV)}$ (Figure 3b), and S_B pertains to the peak area of oxidized peptide **1** generated by *trans*- $[\text{PtCl}_2(\text{en})_2]^{2+}$ (Figure 3c). The relative oxidation yield by $\text{SiO}_2\text{@TPEA@Pt(IV)}$ was calculated to 84%.

Table 1. The sequences of dithiol-containing peptides and the relative oxidation yields.

Peptide Sequence	Relative oxidation yield
1 Ac-CPFC-NH ₂	84%
2 CGYCHKLHQMK-NH ₂	68%
3 CYFQNCPRG-NH ₂ (reduced arginine vasopressin)	68%
4 CRGDKGPDC-NH ₂ (reduced iRGD peptide)	50%
5 CYINQCPLG-NH ₂ (reduced oxytocin)	59%
6 AGCKNFFWKTFTSC (reduced somatostatin)	50%

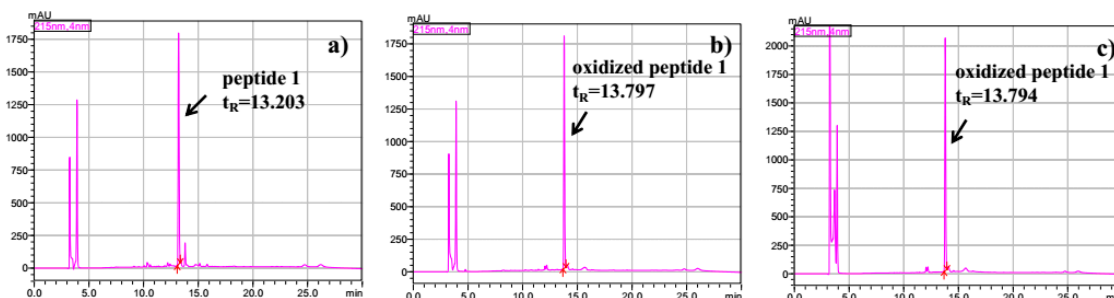


Figure 3. HPLC chromatograms of (a) peptide **1** (1.0 mg/mL, 1.5 mL) after stirring for 30 min; (b) the supernatant from the reaction of $\text{SiO}_2\text{@TPEA@Pt(IV)}$ (50 mg) with peptide **1** (1.0 mg/mL, 1.5 mL) for 30 min; and (c) the mixture from the reaction of $[\text{Pt}(\text{en})_2\text{Cl}_2]\text{Cl}_2$ (1.8 mg) with peptide **1** (1.0 mg/mL, 1.5 mL).

The solid products of the reaction between $\text{SiO}_2\text{@TPEA@Pt(IV)}$ and peptide **1** were separated by centrifugation and washed with DMF and water, and were then oxidized by Cl_2 , regenerating

$\text{SiO}_2@\text{TPEA}@\text{Pt(IV)}$. The reusability of this material for the formation of intramolecular disulfide bond in peptide 1 was examined. No significant decrease in the relative oxidation yield was observed after ten cycles of run (Figure 4). Moreover, the morphology of $\text{SiO}_2@\text{TPEA}@\text{Pt(IV)}$ before and after ten cycles was analyzed by SEM (Figure 5), showing that the $\text{SiO}_2@\text{TPEA}@\text{Pt(IV)}$ nanospheres were still stable after ten cycles of use. On the other hand, $\text{SiO}_2@\text{TPEA}@\text{Pt(II)}$ generated from the reduction of $\text{SiO}_2@\text{TPEA}@\text{Pt(IV)}$ by an excess of peptide 1 was characterized by XPS (Figure 2). A comparison of the XPS spectra of $\text{SiO}_2@\text{TPEA}@\text{Pt(IV)}$ and $\text{SiO}_2@\text{TPEA}@\text{Pt(II)}$ reveals that the peak at a binding energy of 79.56 eV, which is assigned to $\text{Pt(IV)}_{4f(5/2)}$, disappeared in the latter case. This suggests that $\text{SiO}_2@\text{TPEA}@\text{Pt(IV)}$ was reduced thoroughly by peptide 1.

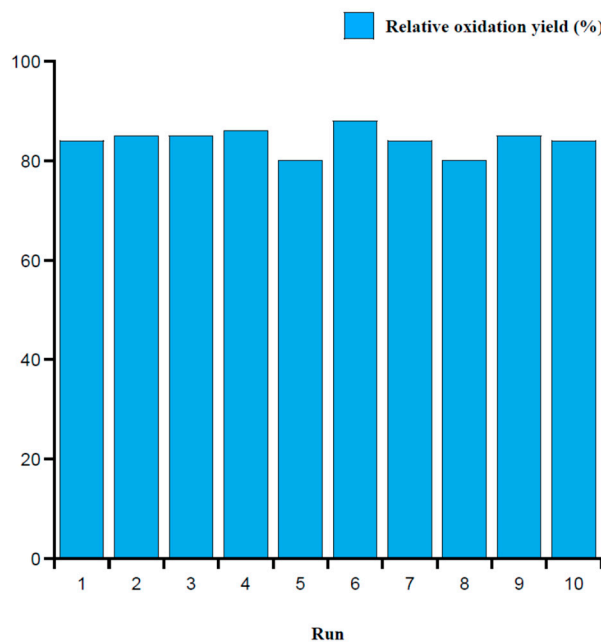


Figure 4. Reusability of $\text{SiO}_2@\text{TPEA}@\text{Pt(IV)}$ over ten reaction cycles.

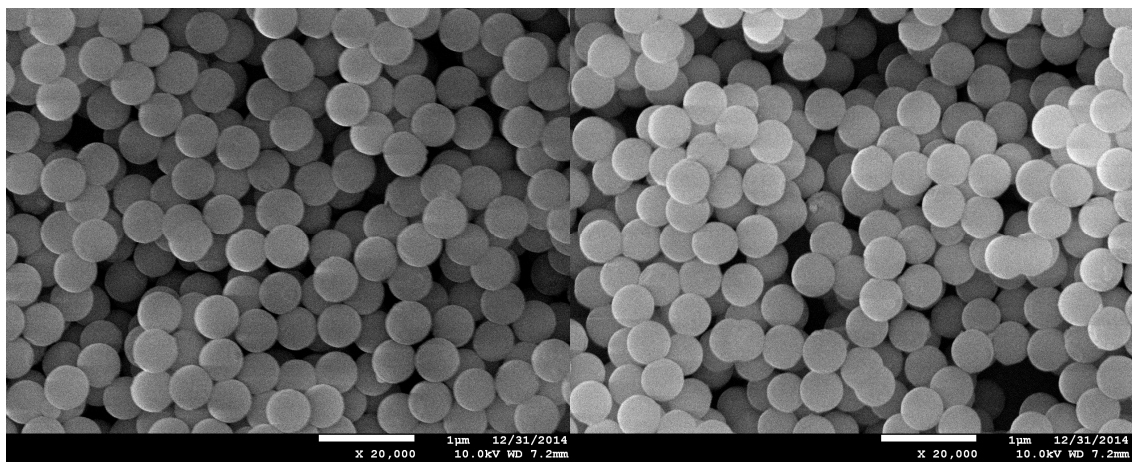


Figure 5. SEM images of $\text{SiO}_2@\text{TPEA}@\text{Pt(IV)}$ before (left) and after being used ten cycles (right).

The role of $\text{SiO}_2@\text{TPEA}@\text{Pt(IV)}$ in the oxidative formation of disulfide bonds in the other five peptides listed in Table 1 was also investigated. The relative oxidation yields for these peptides are given in Table 1. Figures S5-S22 in Supporting Information summarize the reaction conditions, HPLC chromatograms and MS spectra for these reactions. We found that tryptophan, tyrosine and methionine residues were not modified by this oxidant under the conditions used in present work. Also, no dimers were observed in the reactions. Thus, a good selectivity and conversion were

obtained for all the peptides. On the other hand, $\text{SiO}_2@\text{TPEA}@\text{Pt(IV)}$ can be very readily separated from the peptide, and its regeneration is easier than that of $\text{trans-}[\text{PtCl}_2(\text{en})_2]^{2+}$ [36,45].

With reduced oxytocin (peptide 5 in Table 1) as an example, the oxidation property oxytocin of $\text{SiO}_2@\text{TPEA}@\text{Pt(IV)}$ was further investigated. The results are shown in Figures S17a-S17d. The HPLC chromatograms in Fig. S17a and S17b show that the reduced oxytocin was not oxidized significantly by air or by $\text{SiO}_2@\text{TPEA}@\text{Pt(II)}$. Moreover, the peak areas corresponding to reduced oxytocin were essentially the same, demonstrating that the reduced oxytocin is not adsorbed onto $\text{SiO}_2@\text{TPEA}@\text{Pt(II)}$. The HPLC chromatograms for the reactions between the reduced oxytocin and $\text{SiO}_2@\text{TPEA}@\text{Pt(IV)}$ as well as $\text{trans-}[\text{PtCl}_2(\text{en})_2]^{2+}$ are presented in Figure S17c and S17d, showing that there were no significant byproducts formed when the reduced oxytocin was oxidized to oxytocin by $\text{SiO}_2@\text{TPEA}@\text{Pt(IV)}$. On the other hand, the peak area of oxytocin in Figure S23a was similar to that of oxytocin in Figure S23b, demonstrating that $\text{SiO}_2@\text{TPEA}@\text{Pt(II)}$ did not adsorb oxytocin under the reaction conditions.

The oxidation yield was also investigated using the reaction between reduced oxytocin (40 mg) and $\text{SiO}_2@\text{TPEA}@\text{Pt(IV)}$ (0.65 g). After the completion of the reaction, pure oxytocin (24 mg) was obtained as the TFA salt. Thus, the overall disulfide bond formation yield is 60%. On the other hand, the nanospheres containing $\text{SiO}_2@\text{TPEA}@\text{Pt(IV)}$ and $\text{SiO}_2@\text{TPEA}@\text{Pt(II)}$ were washed with pH 4.5 buffer and water. Some sulfur-containing compounds were found to be adsorbed onto the nanospheres and could only be removed using DMF. Unfortunately, the structures of the sulfur-containing compounds are unknown. These sulfur-containing compounds may cause the reaction between $\text{SiO}_2@\text{TPEA}@\text{Pt(IV)}$ and reduced oxytocin to exhibit a lower yield than the reaction between $\text{trans-}[\text{PtCl}_2(\text{en})_2]^{2+}$ and reduced oxytocin.

The reaction between $\text{SiO}_2@\text{TPEA}@\text{Pt(IV)}$ and peptide 5 in different pH buffer solutions (pH 2.0 and 7.1) was also investigated. The relative oxidation yields were between 57% and 65%, which indicate that $\text{SiO}_2@\text{TPEA}@\text{Pt(IV)}$ can also be used for formation of disulfides in peptides in different pH buffers.

The yields for formation of intramolecular disulfide bonds through the oxidation of dithiol-containing peptides by different solid-supported oxidants have been investigated in the literature [15,16]. For example, the oxidation yield in the case of somatostatin was 30% when supported Ellman's reagent was used because a significant amount of peptides was covalently bound to resin beads owing to the disulfide exchange mechanism. For Oxyfold reagent, the overall oxidation yield for the synthesis of disulfide bonds in a model peptide (sequence: H-LCAGPCL-NH₂) was 57%. The oxidation yield was not reported when ChemMatrix-supported NCS was used as the oxidant.¹⁸ In the present work, the oxidation yield for disulfide formation in oxytocin is 60% (the relative oxidation yield is 59%).

3. Experimental procedures

3.1. Materials

Monodispersed silica nanospheres (SiO_2) were obtained as a gift from Dr. Cuimiao Zhang (Hebei University). Fmoc-protected amino acids, Fmoc-Rink-amide-Am resin, and *O*-(benzotriazol-1-yl)-*N,N,N',N'*-tetramethyluronium tetrafluoroborate (HBTU) were purchased from GL Biochem (Shanghai, China). Diisopropylethylamine (DIEA), piperidine, triisopropylsilane, and *N*-[3-(trimethoxysilyl)propyl]ethylenediamine (TPEA), 2,5-dimethoxythiophenol, and $[\text{Pt}(\text{en})_2]\text{Cl}_2$ were purchased from Sigma-Aldrich. Trifluoroacetic acid (TFA), *N,N*-dimethylformamide (DMF), phenol, K_2PtCl_4 , ethylenediamine, and acetonitrile were purchased from Adamas (Tansoole, Shanghai, China). Acetic acid, sodium acetate, ethanol, concentrated HCl, and KMnO_4 were purchased from Shanghai Chemical Reagent Company (Shanghai, China). $[\text{PtCl}_2(\text{en})_2]\text{Cl}_2$ was synthesized according to a method published in the literature [35]. The UV-vis spectrum of the $[\text{PtCl}_2(\text{en})_2]\text{Cl}_2$ solution prepared in this study is in excellent agreement with that reported earlier for $\text{trans-}[\text{PtCl}_2(\text{en})_2]^{2+}$ [35].

3.2. Instrumentation

TEM images of SiO_2 and $\text{SiO}_2@\text{TPEA}$, and EDX data and elemental mapping of $\text{SiO}_2@\text{TPEA}@\text{PtCl}_2$, $\text{SiO}_2@\text{TPEA}@\text{Pt(II)}$, and $\text{SiO}_2@\text{TPEA}@\text{Pt(IV)}$ were recorded on a JEM 2100F transmission electron microscope (JEOL, Japan) at Beihang University. Elemental analysis was conducted to determine the N loading using a CE-440 elemental analyzer (Exeter Analytical Inc., North Chelmsford, MA). The Pt loading on $\text{SiO}_2@\text{TPEA}@\text{Pt(IV)}$ was determined by an X Series 2 ICP-MS system (ThermoFisher, USA). The loading of Pt(IV) complex was determined using a TU-1950 spectrophotometer (Beijing Puxi Inc., Beijing, China) with 1.0 cm quartz cells. SEM images were recorded on a JSM-7500F cold field scanning electron microscope (JEOL, Japan). Fourier transform-infrared (FT-IR) spectra were recorded on a VERTEX 70 FT-IR spectrometer (Bruker, GER) with the KBr pellet technique. X-ray photoelectron spectroscopy (XPS) data for $\text{SiO}_2@\text{TPEA}@\text{Pt(IV)}$ nanospheres were collected on a ESCALAB 250 Xi X-ray photoelectron spectrometer (ThermoFisher, UK). The peptides were synthesized by use of a Focus XC solid phase peptide synthesizer (AAPPTec, USA) and purified on a LC-6AD semi-preparative high performance liquid chromatography (HPLC) system (Shimadzu, Japan) and analyzed on a LC-20AB HPLC system (Shimadzu, Japan).

3.3. Preparation of TPEA-modified silica nanospheres ($\text{SiO}_2@\text{TPEA}$)

$\text{SiO}_2@\text{TPEA}$ was prepared according to a procedure available in the literature [46]. Typically, 1.5 g of SiO_2 was added to 50 mL of dry toluene and the mixture was ultrasonicated for 1 h to obtain a suspension. To the suspension, 2 mL of TPEA was added and the mixture was refluxed for 10 h with stirring under N_2 atmosphere. After cooling to room temperature, the resulting amine-functionalized silica nanospheres ($\text{SiO}_2@\text{TPEA}$) were separated by centrifugation, washed with dry toluene and ethanol, and dried under vacuum.

3.4. Synthesis of $\text{SiO}_2@\text{TPEA}@\text{Pt(IV)}$

Firstly, 1.4 g of $\text{SiO}_2@\text{TPEA}$ was suspended in 50 mL water and ultrasonicated for 1 h. The mixture was heated at 50 °C with stirring under N_2 atmosphere. An aqueous solution of K_2PtCl_4 (0.15 M) was added dropwisely until the supernatant had a slightly yellow color. The resulting platinum complex-modified silica nanospheres ($\text{SiO}_2@\text{TPEA}@\text{PtCl}_2$) were centrifuged and washed with water for several times to remove the unreacted K_2PtCl_4 . Next, $\text{SiO}_2@\text{TPEA}@\text{PtCl}_2$ obtained above was re-dispersed in 50 mL water and ultrasonicated for 30 min; 3 mL of ethylenediamine was added and the resulting mixture was stirred at 100°C for 5 h under N_2 atmosphere. The solid product, which is denoted as $\text{SiO}_2@\text{TPEA}@\text{Pt(II)}$, was centrifuged and washed with water and ethanol, and then dried under vacuum. Finally, 50 mg of $\text{SiO}_2@\text{TPEA}@\text{Pt(II)}$ was suspended in 10 mL of HCl solution (10 mM) and the mixture was ultrasonicated for 10 min. Chlorine gas (generated by the reaction of KMnO_4 with concentrated HCl) was bubbled through the mixture at room temperature for 30 min with stirring, following which N_2 gas was bubbled for an additional 1 h. The silica nanosphere-supported Pt(IV) complex $\{\text{SiO}_2@\text{TPEA}@\text{Pt(IV)}\}$ was centrifuged, washed thoroughly with water and ethanol, and dried under vacuum.

3.5. Determination of Pt(IV) loading in the synthesized $\text{SiO}_2@\text{TPEA}@\text{Pt(IV)}$

3.5.1. Stoichiometry and product analysis

The stoichiometry of the reaction between *trans*- $[\text{PtCl}_2(\text{en})_2]^{2+}$ and 2,5-dimethoxythiophenol was determined in a solution containing a mixture of pH 4.5 buffer and acetonitrile (1:3 v/v) using a TU-1950 spectrophotometer. In these experiments, a series of solutions containing 0.1 mM 2,5-dimethoxythiophenol and various concentrations of *trans*- $[\text{PtCl}_2(\text{en})_2]^{2+}$ (1.96×10^{-2} mM to 0.118 mM) were prepared and kept for 1 h at 25°C. The absorbance values of these solutions were then determined at a wavelength of 330 nm, and the stoichiometry was derived from plots of absorbance versus $[\text{PtCl}_2(\text{en})_2^{2+}]$. To analyze the product obtained from the reaction between 2,5-dimethoxythiophenol and *trans*- $[\text{PtCl}_2(\text{en})_2]^{2+}$, the reaction mixture composed of 1.0 mM *trans*- $[\text{PtCl}_2(\text{en})_2]^{2+}$ and 2.0 mM 2,5-dimethoxythiophenol was dissolved in a solution containing a mixture

of pH 4.5 buffer and acetonitrile (1:3 v/v) and kept for 1 h at 25°C. This solution was then analyzed using an ESI-MS spectrometer.

3.5.2. Determination of Pt(IV) loading in $\text{SiO}_2@\text{TPEA}@\text{Pt(IV)}$

All the solutions were prepared in a pH 4.5 buffer/acetonitrile (1:3 v/v) mixtures. 2,5-dimethoxythiophenol solution (0.5 mL, 20.0 mM) was mixed with *trans*-[PtCl₂(en)₂]²⁺ (2.5 mL, 3 mM) and diluted to 5.0 mL. After reaction for 1 h, the mixture was further diluted to 2,5-dimethoxythiophenol disulfide concentrations of 0.025, 0.05, 0.10, 0.15, 0.20, 0.25, and 0.3 mM, and absorbance values were measured at 330 nm. The experiments were performed in triplicate and a calibration curve of absorbance as a function of concentration was prepared. Next, $\text{SiO}_2@\text{TPEA}@\text{Pt(IV)}$ (25 mg) was placed in a solution containing 2,5-dimethoxythiophenol (2 mL, 5.0 mM) and the mixture was shaken for 1 h at room temperature and centrifuged. The supernatant (0.5 mL) was diluted to 5 mL. An absorbance value of 0.56 was obtained, corresponding to a Pt(IV) loading of 0.15 mmol/g.

3.6. Disulfide bond formation in peptides

3.6.1. Synthesis and purification of peptides

Peptides were synthesized by means of a Focus XC solid phase peptide synthesizer using the standard Fmoc methodology [47]. Fmoc-Rink-amide resin (0.66 mmol/g, 250 mg) was used for the synthesis of the peptides. All the coupling reactions were carried out using 3 mL of amino acid (0.33 mM) in DMF, 3 mL of HBTU (0.33 M) in DMF, and 2 mL of DIEA (1.0 M) in DMF for 50 min. Fmoc deprotection was performed with a 20% piperidine DMF solution. A cleavage cocktail containing 4% phenol, 2% water, 2% triisopropylsilane, and 92% TFA was used to cleave the peptides from the resin. After the resin was removed by filtration, the filtrate was treated with diethyl ether, and the peptides were separated by centrifugation and dissolved in water. Crude peptides were obtained after lyophilization. The peptides were purified by semi-preparative RP-HPLC system equipped with a UV-vis detector at 215 nm using a 250 mm x 20 mm ODS-C₁₈ column at a flow rate of 10 mL/min. Two solvent systems consisting of 0.03% TFA in acetonitrile and 0.03% TFA in water (referred to as solvents A and B) were used for peptide elution with a suitable gradient. After lyophilization, the peptides were obtained as TFA salts and used for further experiments.

3.6.2. General method of disulfide formation

An excess of $\text{SiO}_2@\text{TPEA}@\text{Pt(IV)}$ was added to a peptide solution and the mixture was stirred for 30 min at 25°C, followed by centrifugation to remove the nanospheres. The solution obtained was analyzed using a gradient RP-HPLC system equipped with a UV-vis detector at 215 nm using a 250 mm x 4.6 mm C₈ column at a flow rate of 1.0 mL/min. The solvent system encompassed A (0.03% or 0.1% TFA in acetonitrile) and B (0.03% or 0.1% TFA in water).

4. Conclusions

$\text{SiO}_2@\text{TPEA}@\text{Pt(IV)}$ was synthesized successfully and used for formation of disulfide in six dithiol-containing peptides. The concept of “relative oxidation yield” was defined and used to evaluate the efficiency of disulfide formation in these peptides. $\text{SiO}_2@\text{TPEA}@\text{Pt(IV)}$ is stable and can be used at least ten cycles without any decrease in the relative oxidation yield. The overall yield is 60% for the oxidative synthesis of oxytocin by this oxidant. However, the reason for the low yield during the synthesis of oxytocin is unclear. We intend to investigate the reason for the low yield in the future, which can aid in the efficient synthesis of disulfide bonds in peptides.

Acknowledgments: Financial support to this work by grants from National Natural Science Foundation of China (21406047), Natural Science Foundation of Hebei Province (B2016201014), and Natural Science Foundation of Educational Commission of Hebei Province (ZD2016073) are gratefully acknowledged. We thank Professor Tiesheng Shi for critically reading and correcting the manuscript.

Author Contributions: Shuying Huo and Shigang Shen conceived and designed the experiments; Xiaonan Hou and Xiaowei Zhao performed the experiments; Xiaonan Hou and Yamei Zhang analyzed the data; Aying Han contributed reagents/materials/analysis tools; Shuying Huo and Shigang Shen wrote the paper.

Conflicts of Interest: The authors declare no conflict of interest.

References

1. Gongora-Benitez, M.; Tulla-Puche, J.; Albericio, F. Multifaceted Roles of Disulfide Bonds. Peptides as Therapeutics. *Chem Rev.* **2014**, *114*, 901-926.
2. Northfield, S.E.; Wang, C.K.; Schroeder, C.I.; Durek, T.; Kan, M.W.; Swedberg, J.E.; Craik, D.J. Disulfide-rich macrocyclic peptides as templates in drug design. *Eur. J. Med. Chem.* **2014**, *77*, 248-257.
3. Chen, S.; Gopalakrishnan, R.; Schaer, T.; Marger, F.; Hovius, R.; Bertrand, D.; Pojer, F.; Heinis, C. Dithiol amino acids can structurally shape and enhance the ligand-binging properties of polypeptides. *Nature Chem.* **2014**, *6*, 1009-1016.
4. Zompa, A.A.; Galanis, A.S.; Werbitzky, O.; Albericio, F. Manufacturing peptides as active pharmaceutical ingredients. *Future Med. Chem.* **2009**, *1*, 361-377.
5. Mandal, B.; Basu, B. Recent advances in S-S bond formation. *RSC Adv.* **2014**, *4*, 13854-13881.
6. Postma, T.M.; Albericio, F. Disulfide Formation Strategies in Peptide Synthesis. *Eur. J. Org. Chem.* **2014**, 3519-3530.
7. Bulaj, G. Formation of disulfide bonds in proteins and peptides. *Biotech. Adv.* **2005**, *23*, 87-92.
8. Kudryavtseva, E.V.; Sidorova, M.V.; Evstigneeva, R.P. Some peculiarities of synthesis of cysteine-containing peptides. *Russ. Chem. Rev.* **1998**, *67*, 545-562.
9. Annis, I.; Hargittai, B.; Barany, G. Disulfide Bond Formation in Peptides. *Method Enzymol.* **1997**, *289*, 198-221.
10. Shi, T.S.; Rabenstein, D.L. *trans*-Dichlorotetracyanoplatinate(IV) as a Reagent for the Rapid and Quantitative Formation of Intramolecular Disulfide Bonds in Peptides. *J. Org. Chem.* **1999**, *64*, 4590-4595.
11. Shi, T.S.; Rabenstein, D.L. Discovery of a Highly Selective and Efficient Reagent for Formation of Intramolecular Disulfide Bonds in Peptides. *J. Am. Chem. Soc.* **2000**, *122*, 6809-6815.
12. Shi, T.S.; Rabenstein, D.L. Formation of multiple intramolecular disulfide bonds in peptides using the reagent *trans*-[Pt(ethylenediamine)₂Cl]²⁺. *Tetrahedron Lett.* **2001**, *42*, 7203-7206.
13. Shi, T.S.; Rabenstein, D.L. Convenient Synthesis of Human Calcitonin and Its Methionine Sulfoxide Derivative. *Bioorg. Med. Chem. Lett.* **2002**, *12*, 2237-2240.
14. Nguyen, K.; Iskandar, M.; Rabenstein, D. L. Kinetics and Equilibria of Cis/Trans Isomerization of Secondary Amide Peptide Bonds in Linear and Cyclic Peptides. *J. Phys. Chem. B* **2010**, *114*, 3387-3392.
15. Postma, T.M.; Albericio, F. *N*-chlorosuccinimide, an efficient peptide disulfide bond-forming reagent in aqueous solution. *RSC Adv.* **2013**, *3*, 14277-12280.
16. Postma, T.M.; Albericio, F. *N*-chlorosuccinimide, an efficient for on-resin disulfide formation in solid-phase peptide synthesis. *Org. Lett.* **2013**, *15*, 616-619.
17. Arai, A.; Dedachi, K.; Iwaoka, M. Rapid and quantitative disulfide bond formation for a polypeptide chain using a cyclic selenoxide reagent in an aqueous medium. *Chem. Eur. J.* **2011**, *17*, 481-485.
18. Postma, T.M.; Albericio, F. Disulfide formation strategies in peptide synthesis. *Eur. J. Org. Chem.* **2014**, *17*, 3519-3530.
19. Annis, I.; Chen, L.; Barany, G. Novel Solid-Phase Reagents for Facile Formation of Intramolecular Disulfide Bridges in Peptides under Mild Conditions. *J. Am. Chem. Soc.* **1998**, *120*, 7226-7238.
20. Verdie, P.; Ronga, L.; Cristau, M.; Amblard, M.; Cantel, S.; Enjalbal, C.; Puget, K.; Martinez, J.; Subra, G. Oxyfold: A Simple and Efficient Solid-Supported Reagent for Disulfide Bond Formation. *Chem. Asian J.* **2011**, *6*, 2382-2389.
21. Ronga, L.; Verdie, P.; Sanchez, P.; Enjabal, C.; Maurras, A.; Jullian, M.; Puget, K.; Martinez, J.; Subra, G. Supported oligomethionine sulfoxide and Ellman's reagent for cysteine bridges formation. *Amino Acids*, **2013**, *44*, 733-742.
22. Postma, T.M.; Albericio, F. Immobilized *N*-Chlorosuccinimide as a Friendly Peptide Forming Reagent. *ACS Comb. Sci.* **2014**, *16*, 160-163.
23. Rimoldi, M.; Mezzetti, A. Site isolated complexes of late transition metals grafted on silica: challenges and chances for synthesis and catalysis. *Catal. Sci. Technol.* **2014**, *4*, 2724-2740.

24. Conley, M.P.; Coperet, C.; Thieuleux, C. Mesostructured Hybrid Organic-Silica Materials: Ideal Supports for Well-Defined Heterogeneous Organometallic Catalysts. *ACS Catal.* **2014**, *4*, 1458-1469.
25. Sharma, R.K.; Sharma, S.; Dutta, S.; Zboril, R.; Gawande, M.B. Silica-nanosphere-based organic-inorganic hybrid nanomaterials: synthesis, functionalization and applications in catalysis. *Green Chem.* **2015**, *17*, 3207-3230.
26. Sharma, R.K.; Sharma, S. Silica nanosphere-supported palladium(II) furfural complex as a highly efficient and recyclable catalyst for oxidative amination of aldehydes. *Dalton Trans.* **2014**, *43*, 1292-1304.
27. Atar, A.B.; Kim, J.S.; Lim, K.T.; Jeong, Y.T. Bridging homogeneous and heterogeneous catalysis with CAN-SiO₂ as a solid catalyst for four component reactions for the synthesis of tetrasubstituted pyrroles. *New. J. Chem.* **2015**, *39*, 396-402.
28. Sharma, P.; Singh, A.P. A covalently anchored 2,4,6-triallyloxy-1,3,5-triazine Pd(II) complex over a modified surface of SBA-15: catalytic application in hydrogenation reaction. *RSC Adv.* **2014**, *4*, 58467-58475.
29. Stoeber, W.; Fink, A.; Bohn, E. Controlled growth of monodisperse silica spheres in the micron size range. *J. Colloid Interface Sci.* **1968**, *26*, 62-69.
30. Ma, Q.; Li, Y.; Su, X. Silica-nanobead-based sensors for analytical and bioanalytical applications. *Trends in Anal. Chem.* **2015**, *74*, 130-145.
31. Zheng, F.; Hu, B. Preparation of a high pH-resistant AAPTS-silica coating and its application to capillary microextraction (CME) of Cu, Zn, Ni, Hg and Cd from biological samples followed by on-line ICP-MS detection. *Anal. Chim. Acta*, **2007**, *605*, 1-10.
32. Chaudhary, Y.S.; Ghatak, J.; Bhatta, U.M.; Khushalani, D. One-step method for the self-assembly of metal nanoparticles onto faceted hollow silica tubes. *J. Mater. Chem.* **2006**, *16*, 3619-3623.
33. He, Y.; Huang, Y.; Jin, Y.; Liu, X.; Liu, G.; Zhao, R. Well-Defined Nanostructured Surface-Imprinted Polymers for Highly Selective Magnetic Separation of Fluoroquinolones in Human Urine. *ACS Appl. Mater. Interfaces*, **2014**, *6*, 9634-9642.
34. Robillard, M.S.; Valentijn, A. Rob. P.M.; Meeuwenoord, N.J.; van der Marel, G.A.; van Boom, J.H.; Reedijk, J. The First Solid-Phase Synthesis of a Peptide-Tethered Platinum(II) Complex. *Angew. Chem. Int. Ed.* **2000**, *39*, 3096-3099.
35. Robillard, M.S.; Bacac, M.; van den Elst, H.; Flamigni, A.; van der Marel, G.A.; van Boom, J.H.; Reedijk, J. Automated Parallel Solid-Phase Synthesis and Anticancer Screening of a Library of Peptide-Tethered Platinum(II) Complexes. *J. Comb. Chem.* **2003**, *5*, 821-825.
36. Basolo, F.; Jr Bailar, J.C.; Tarr, B.R. The Stereochemistry of Complex Inorganic Compounds. X. The Stereoisomers of Dichlorobis-(ethylenediamine)-platinum(IV) Chloride. *J. Am. Chem. Soc.* **1950**, *72*, 2433-2438.
37. Watt, G.W.; Thompson, Jr J.S. Deprotonation of 2-(2-aminoethylamino)ethanol complexes of platinum(II), IV) and palladium(II) with liquid ammonia and potassium amide. *J. Inorg. Nucl. Chem.* **1974**, *36*, 1075-1078.
38. Liang, B.; Huo, S.; Ren, Y.; Sun, S.; Cao, Z.; Shen, S. A. platinum(IV)-based metallointercalator: synthesis, cytotoxicity, and redox reactions with thiol-containing compounds. *Transition Met. Chem.* **2015**, *40*, 31-37.
39. Wilson, J. J.; Lippard, S. J. Synthetic Methods for the Preparation of Platinum Anticancer Complexes. *Chem. Rev.* **2014**, *114*, 4470-4495.
40. Hall, M.D.; Mellor, H.R.; Callaghan, R.; Hambley, T.W. Basis for Design and Development of Platinum(IV) Anticancer Complexes. *J. Med. Chem.* **2007**, *50*, 3403
41. Kolbeck, C.K.; Taccardi, N.; Paape, N.; Schulz, P.S.; Wasserscheid, P.; Steinruck, H.P.; Maier, F. R Redox chemistry, solubility, and surface distribution of Pt(II) and Pt(IV) complexes dissolved in ionic liquids. *J. Mol. Liq.* **2014**, *192*, 103-113.
42. Burroughs P.; Hamnett A.; McGilp J.F.; Orchard A.F. Radiation damage in some platinum(IV) complexes produced during soft X-ray photoelectron spectroscopic studies. *J. Chem. Soc., Faraday Trans. 2*, **1975**, *71*, 177-187.
43. Ling, X.; Shen, Y.; Sun, R.; Zhang, M.; Li, C.; Mao, J.; Xing, J.; Sun, C.; Tu, J. Tumor-targeting delivery of hyaluronic acid-platinum(IV) nanoconjugate to reduce toxicity and improve survival. *Polymer Chem.* **2015**, *6*, 1541-1552.
44. Lengke, M.F.; Fleet, M.E.; Southam G. Synthesis of Platinum Nanoparticles by Reaction of Filamentous Cyanobacteria with Platinum(IV)-Chloride Complex. *Langmuir*, **2006**, *22*, 7318-7323.
45. Lu, Y.; Hou, X.; Zhao, X.; Liu, M.; Shen, F.; Ren, Y.; Liu, Y.; Huo, S.; Shen, S. Kinetics and mechanism of oxidation of 3,6-dioxa-1,8-octanedithiol and DL-dithiothreitol by a platinum(IV) complex. *Transition Met. Chem.* **2016**, *41*, 45-55.

46. Chaudhary, Y.S.; Ghatak, J.; Bhatta, U.M.; Khushalani, D. One-step method for the self-assembly of metal nanoparticles onto faceted hollow silica tubes. *J. Mater. Chem.* **2006**, *16*, 3619–3623.
47. Coantic, S.; Subra, G.; Martinez J. Microwave-assisted Solid Phase Peptide Synthesis on High Loaded Resins. *Int. J. Pept. Res. Ther.* **2008**, *14*, 143–147.

Sample Availability: Samples of the compounds are available from the authors.



© 2016 by the authors; licensee Preprints, Basel, Switzerland. This article is an open access article distributed under the terms and conditions of the Creative Commons by Attribution (CC-BY) license (<http://creativecommons.org/licenses/by/4.0/>).